

Gravitational-Wave Implications for the Parity Symmetry of Gravity at GeV Scale

Yifan Wang

Max Planck Institute for Gravitationalphysics <https://orcid.org/0000-0002-2928-2916>

Rui Niu

University of Science and Technology of China

Wen Zhao (✉ wzhao7@ustc.edu.cn)

University of Science and Technology of China

Tao Zhu

Zhejiang University of Technology <https://orcid.org/0000-0003-2286-9009>

Article

Keywords: gravitational-wave astronomy, parity symmetry, GeV Scale

Posted Date: August 27th, 2020

DOI: <https://doi.org/10.21203/rs.3.rs-57578/v1>

License: © ⓘ This work is licensed under a Creative Commons Attribution 4.0 International License.

[Read Full License](#)

Gravitational-Wave Implications for the Parity Symmetry of Gravity at GeV Scale

Yi-Fan Wang^{1,2}, Rui Niu^{3,4}, Tao Zhu^{5,6}, Wen Zhao^{3,4,*}

¹Max-Planck-Institut für Gravitationsphysik (Albert-Einstein-Institut), D-30167 Hannover, Germany ²Leibniz Universität Hannover, D-30167 Hannover, Germany ³CAS Key Laboratory for Research in Galaxies and Cosmology, Department of Astronomy, University of Science and Technology of China, Hefei 230026, China ⁴School of Astronomy and Space Sciences, University of Science and Technology of China, Hefei, 230026, China ⁵Institute for theoretical physics and Cosmology, Zhejiang University of Technology, Hangzhou, 310032, China ⁶United center for gravitational wave physics (UCGWP), Zhejiang University of Technology, Hangzhou, 310032, China *wzhao7@ustc.edu.cn

Einstein's general relativity, as the most successful theory of gravity, is one of the cornerstones of modern physics. However, the experimental tests for gravity in the high energy region are limited. The emerging gravitational-wave astronomy has opened an avenue for probing the fundamental properties of gravity in strong and dynamical field, and in particular, high energy regime. In this work, we focus on the parity symmetry of gravity. For broken parity, the left- and right-handed modes of gravitational waves would follow different equations of motion, dubbed as birefringence. We perform the first full Bayesian inference of the parity conservation of gravity by comparing the state-of-the-art waveform with the compact binary coalescence data released by LIGO and Virgo collaboration. We do not find any violations of general relativity, thus obtain the lower bound of the parity-violating energy scale to be 0.09 GeV through the velocity birefringence of gravitational waves. This provides the most stringent experimental test of gravitational parity symmetry up to date, and for the first time, in the high energy region, which ushers in a new era of using gravitational waves to test the ultraviolet behavior of gravity. We also find third-generation gravitational-wave detectors can enhance this bound to $\mathcal{O}(10^2)$ GeV if there is still no violation, comparable to the current Large Hadron Collider (LHC) energy scale in particle physics.

Symmetry is an essential characteristic of the fundamental theories of modern physics and thus must be tested experimentally. In this work, we focus on testing the parity symmetry which indicates the invariance of physical laws under reversed spatial coordinates. It is well-known that parity is conserved for strong and electromagnetic interactions but is broken in the weak interaction as firstly confirmed by the beta-decay experiment in cobalt-60^{1,2}. Gravitational parity is conserved in Einstein's general relativity (GR). Nevertheless, various parity-violating gravity models, including Chern-Simons gravity³, ghost-free scalar-tensor gravity⁴, the symmetric teleparallel equivalence of GR theory⁵ and Hořava-Lifshitz gravity^{6,7} have been proposed for different motivations such as gravity quantization. In particular, in some fundamental theories of gravity, such as string theory and loop quantum gravity, the parity violation in the high energy regime is inevitable³. However, the observational evidence for gravity in the *high energy* scale is limited, which leaves the gravitational wave (GW) observations as a last resort⁸⁻¹⁰. In contrast to the tests of the Solar system or binary pulsars, GW reflects the wave behavior of the gravitational field. Therefore, the tiny deviation from GR, if exists, could be accumulated and magnified during propagation of GWs. In this work, we report the first full Bayesian analysis for gravitational parity conservation at sub-GeV scale from

the GW observation, which demonstrates the feasibility of probing the *high energy* behavior of gravity through GWs.

We first construct the generalized GW waveform generated by compact binary coalescence (CBC) with parity violation within the effective field theory (EFT) formalism. EFT provides a systematic framework to encode all kinds of modifications to an existing theory that could arise given certain new physics, thus simultaneously testing a range of modified gravity theories at once. To investigate the possible propagation effect due to parity violation, we consider the perturbation theory of gravitational field. EFT suggests that the leading-order modification to the GR linearized action comes from two terms with three derivatives, i.e., $\epsilon^{ijk} \dot{h}_{il} \partial_j \dot{h}_{kl}$ and $\epsilon^{ijk} \partial^2 h_{il} \partial_j h_{kl}$ with ϵ^{ijk} the antisymmetric symbol and h_{ij} the tensor perturbation of metric, ∂_j and a *dot* denote the derivatives with respect to spatial coordinates and time, respectively¹¹, ∂^2 is the Laplacian, $i, j, \dots = 1, 2$ or 3 refer to spatial coordinate. Both terms are parity-violating. Dimensional analysis dictates that these new terms are each suppressed by an energy scale. We expect the two energy scales are of the same order, and denote collectively by M_{PV} . Otherwise, if the two energy scales differ by orders of magnitude, only the term with lower energy scale dominates, thus we can neglect another term and our result for M_{PV} will not change (see *Methods*). This EFT with leading-order extensions to GR can be mapped to all the existing specific parity-violating modified gravity models in the market¹². Also note that since parity violation emerges at the leading order modification, we expect the most stringent test on gravity from the propagation of GW, at least from the viewpoint of EFT, is on the gravitational parity symmetry.

As demonstrated by Ref.¹³, the modifications to GR-based GW waveform only arise from the propagation effect given the leading order parity violation modification discussed above, because the generation effect occurs on a radiation-reaction timescale much smaller than the GW time of flight and its impact on the evolution of the GW waveform is negligible. Given the parity-violating terms, the equation of motion for the GW circular polarization mode h_A in a Friedmann-Robertson-Walker (FRW) universe is

$$h_A'' + (2 + \nu_A)\mathcal{H}h_A' + (1 + \mu_A)k^2 h_A = 0, \quad (1)$$

where $A = L$ or R stands for the left- and right-hand modes, \mathcal{H} is the conformal Hubble parameter, k is the wave-number, a *prime* denotes the derivative with respect to the conformal cosmic time. Note that $\mu_A = \nu_A = 0$ would reduce Eq. (1) to GR. Dimensional analysis indicates that both terms relate to the energy scale M_{PV} by $\mu_A \propto \rho_{Ak}/M_{PV}$ and $\nu_A \propto \rho_{Ak}/M_{PV}$ with $\rho_R = 1$ and $\rho_L = -1$. The broken parity leads to asymmetry between the left- and right-hand circular polarization modes of GW during propagation. In particular, the opposite sign of μ_A (as well as ν_A) for different modes leads to the birefringence effect of GWs, which is a characterized phenomenon for GW propagation in the parity-violating gravity. We find that the propagation of GWs can be affected in two ways. The term μ_A modifies the conventional dispersion relation of GWs. As a result, the velocities of left- and right-hand circular polarization of GWs are different, dubbed as the *velocity birefringence* of GW¹⁴. On the other hand, the term ν_A induces the different damping rates for two polarization modes when they propagate in the expanding Universe, which is called the *amplitude birefringence* of GWs¹³. In the general parity-violating gravity

108 theories, both effects exist. For each circular polarization mode, the
 109 former effect exactly induces the phase modifications of the GW wave-
 110 form, and the latter one induces the amplitude modifications. Con-
 111 straints on modification of equation of motion with form Eq. (1) are
 112 also obtained by LIGO and Virgo collaboration in Ref. ¹⁵, but only
 113 parity conserving terms are considered. In contrast, our work focus
 114 on the parity-violating effect. Note that, in EFT, the next-to-leading
 115 order modification terms in the action, which are leading-order parity-
 116 conserving terms, also follow the Eq.(1) with $\nu_A \propto (k/M_{\text{PV}})^2$ and
 117 $\mu_A \propto (k/M_{\text{PV}})^2$ ^{11,12,14}. Therefore, their effects on the GW waveform
 118 are much smaller than the parity-violating effects.

119 From the equation of motion, one can derive the parity-violating
 120 GW waveform in the frequency domain, which is

$$h_A^{\text{PV}}(f) = h_A^{\text{GR}}(f) (1 + \rho_A \delta h) e^{i\rho_A \delta \Psi}, \quad (2)$$

121 where f is the frequency, and the amplitude modification δh and the
 122 phase modification $\delta \Psi$ are induced by ν_A and μ_A , respectively. It
 123 should also be noted that since $\delta \Psi$ is larger than δh by about 20
 124 order of magnitude (see Methods), it is safe to only take into account the
 125 contribution of $\delta \Psi$. But we also consider a special scenario where the
 126 velocity birefringence is forbidden, i.e., $\delta \Psi = 0$ as is the case for, e.g.,
 127 Chern-Simons gravity.

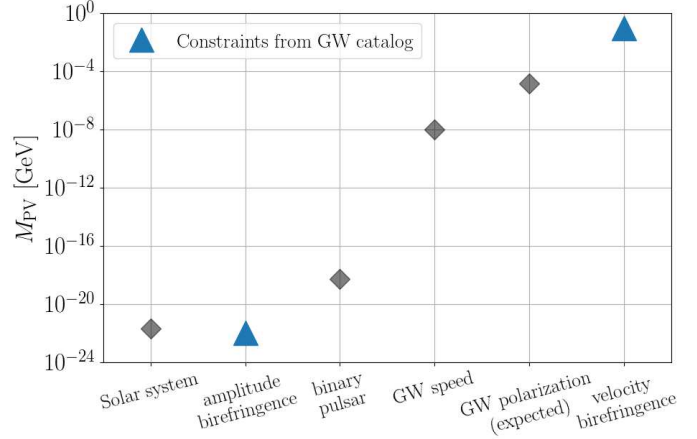
128 With the waveform in Eq. (2), we can perform a direct comparison
 129 with the GW data using Bayesian inference to test the parity violation.
 130 Up to date, LIGO and Virgo collaborations have released the data of
 131 confident CBC events from the first and second observation run. The
 132 catalog GWTC-1 include ten binary black hole (BBH) events and a
 133 binary neutron star (BNS) event GW170817 ¹⁶. Recently, a second
 134 BNS event, GW190425, has been released ¹⁷. We analyze the open
 135 data ¹⁸ of the twelve events with the inference module of the open-
 136 source software PyCBC ¹⁹ developed for GW astronomy, which in turn
 137 has dependency on LALSuite ²⁰.

138 For all the GW events, we do not find any signatures of parity viola-
 139 tion. We thus put the lower limit of M_{PV} to be 0.09 GeV in the general
 140 parity-violating gravity. This is tighter than the Solar system tests and
 141 the binary pulsar observation by 17 orders of magnitude. The reason
 142 for this dramatic improvement is that the velocity birefringence effect
 143 in the modification of GW waveform is accumulated during the prop-
 144 agation of GW signals, and can be greatly amplified for distant GW
 145 events. We note that this result has direct application on constraining a
 146 range of specific parity-violating gravity models with velocity birefring-
 147 ence, including the ghost-free scalar-tensor gravity ⁴, the symmetric
 148 teleparallel equivalence of GR theory ⁵ and Hořava-Lifshitz gravity ^{6,7}.
 149 The detailed correspondence between the above modified gravity mod-
 150 els and the EFT formalism can be found in Ref. ¹². We have made
 151 our inference results open to facilitate mapping the constraint to any
 152 specific parity-violating gravity theories that one is interested in.

153 By similar analysis, the constraint by only considering the ampli-
 154 tude birefringence modification is $M_{\text{PV}} > 1 \times 10^{-22}$ GeV. This result
 155 can be directly compared to and is consistent with Refs. ^{13,21,22} which
 156 focuses on testing Chern-Simons gravity with GW. Compared to the
 157 constraint from velocity birefringence, the loose result for amplitude
 158 birefringence is because δh is negligibly small compared to $\delta \Psi$ and the
 159 GW detection is less sensitive to amplitude modification than phase.

160 Our results of the constraint on M_{PV} are shown in Fig. 1, where
 161 we have combined the results from the twelve CBC events to give an
 162 overall constraint. Other existing constraints including the Solar system
 163 tests and the binary pulsar observation are also plotted for comparison.

164 With the continuing sensitivity upgrade during the advanced LIGO
 165 and Virgo runs, the future GW astronomy is even more powerful to
 166 test the parity symmetry of gravity. The KAGRA detector has joined
 167 the global network very recently. The advanced LIGO and Virgo detec-
 168 tors are expected to achieve the design sensitivity in a few years ²⁶.



169 **Figure 1 | Current constraints on the lower limits of parity-violating energy**
 170 **scales in gravity from various observations.** The triangle markers denote the
 171 constraints from the GW catalog for the general parity-violating gravity with ve-
 172 locity birefringence and the special case with only amplitude birefringence, re-
 173 spectively. For comparison, the figure also includes the results from the LA-
 174 GEOS satellite in the Solar system ²³, that from the double pulsar system PSR
 175 J0737-3039 A/B ²⁴, that from the arrival time difference between GW170817 and
 176 GRB170817A, and the potential result by considering the waveform-independent
 177 method developed in Ref. ²⁵.

178 The third generation ground-based GW detectors, including the Ein-
 179 stein Telescope and the Cosmic Explorer, are under projection currently
 180 ²⁷. We investigate the ability of future GW astronomy to constrain the
 181 lower limit of M_{PV} by simulations. With one-year observation time,
 182 M_{PV} is expected to be constrained to be no less than $\mathcal{O}(1)$ GeV with
 183 the second generation detectors with designed sensitivity and $\mathcal{O}(10^2)$
 184 GeV with the projected third generation detectors. This is compara-
 185 ble with the existing *high energy* experiments in particle physics from
 186 LHC. These results indicate that, through GW observations, for the first
 187 time it becomes feasible to test the ultraviolet behavior of gravity in the
 188 *high energy* region experimentally.

189 We note that other constraints on the violation of parity symme-
 190 try of gravity have also been derived in various analysis using GW or
 191 non-GW observations. In the following, we briefly summarize these
 192 results to describe the status-of-the-art of the constraint on M_{PV} . The
 193 results are also presented in Fig. 1 as a comparison of this work. Com-
 194 pared to the following constraints which also use GW, one major dif-
 195 ference is that our work makes use of the inspiral-merger-ringdown
 196 parity-violating GW waveform (Eq. (2)) which represents the maxi-
 197 mum information that can be extracted from the signal. In addition, the
 198 Bayesian nature of our method allows for combining the results from a
 199 catalog of events.

200 **Waveform-independent constraint from GWs:** Our previous work
 201 Ref. ²⁵ develops a waveform-independent way to decompose the left-
 202 and right-hand polarization modes from the observed GW data if the
 203 sky position of the event can be fixed by the observation of its elec-
 204 tromagnetic counterparts. From the frequency-time representations we
 205 can read out the arrival times of GW in each frequency band. Ac-
 206 cording to the velocity birefringence effect, for a specific frequency
 207 f , the arrival time difference between the two modes is $|t_{R-L}| =$
 208 $(2\pi f/M_{\text{PV}})^2 \int_{t_e}^{t_0} a^{-2} dt$ ²⁵, where a is the scale factor of the Universe,
 209 t_0 and t_e are the cosmic time of the arrival and the emission of the GW
 210 event respectively. This formula gives a direct relation between the ar-
 211 rival time difference and the energy scale of parity violation M_{PV} . Ap-
 212 plying to the mock data, we find that if a nearly edge-on BNS at 40 Mpc
 213 is detected by the second-generation detector network consisting of ad-
 214 vanced LIGO, advanced Virgo, KAGRA, and LIGO-India, one could

206 derive the waveform-independent bound $M_{\text{PV}} > 1.4 \times 10^4$ eV. At
 207 this writing, the BNS signal GW170817 is the unique GW event with
 208 observed electromagnetic counterparts. However, this event is nearly
 209 face-on with the inclination angle $\iota \geq 152^\circ$ ²⁸, thus the right-hand
 210 mode of this event is completely dominant. Therefore, the difference
 211 of the arrival time between the two modes cannot be determined from
 212 GW170817.

213 *Constraint from GW speed:* The velocity birefringence effect of
 214 GW can be constrained from the speed of GW, which in turn can
 215 be obtained by comparing the arrival time of GW signal and that of
 216 the electromagnetic signal. For the event GW170817/GRB170817A,
 217 the arrival time difference between GW and gamma-ray burst is 1.7
 218 seconds. Assuming the difference of their emission time is less than
 219 10 seconds, the speed of the right-hand circular mode of GW is in
 220 the range $-7 \times 10^{-16} < 1 - v_R < 3 \times 10^{-15}$ ²⁹. According to
 221 the relation $|v_R - 1| = \pi f / M_{\text{PV}}$ ¹², one obtains the constraint
 222 $M_{\text{PV}} \gtrsim 10$ eV. This is consistent with the result in Ref.³⁰, where the
 223 authors focus on the ghost-free scalar-tensor gravity models with parity
 224 violation. Bounds on GW birefringence were also obtained in Ref.
 225 ¹⁴ with GW150914 for testing local Lorentz invariance by identifying
 226 the speed difference between two polarization modes. We note that our
 227 EFT formulation can be mapped to the formulation proposed in Ref.
 228 ^{14,31}, more detailed analysis is beyond the scope of this work and thus
 229 leave as a future work.

230 *Constraint from Solar system tests:* In the parity-violating gravi-
 231 ty, an important feature is that it leads to a change of frame-dragging
 232 effects around rotating objects, which can be used to test the theory.
 233 Focusing on the Chern-Simons gravity, Ref.²³ calculates the linearized
 234 metric of the spacetime around a non-relativistic, constant-density spin-
 235 ning body. It is found that the gravitomagnetic field in the parity-
 236 violating gravity differs from that in GR, which induces the modifica-
 237 tions in the precession of orbits of gyroscopes moving in this space-
 238 time. Using the measurement of Lense-Thirring drag around the Earth
 239 by the LAGEOS satellites, Ref.²³ sets the constraint on the character-
 240 istic Chern-Simons length scale, $k_{\text{CS}}^{-1} \lesssim 1000$ km, which corresponds
 241 to $M_{\text{PV}} \gtrsim 2 \times 10^{-13}$ eV.

242 *Constraint from binary pulsar:* In the parity-violating gravity, the
 243 theory selects a preferred direction in spacetime that corrects the pre-
 244 cession of the orbital plane. Thus, observations of gravitomagnetic
 245 precession can be used to test the validity of the theory. In Refs.^{24,32},
 246 the authors focus on the Chern-Simons modified gravity with a time-
 247 like Chern-Simons coupling scalar field, and calculate the leading-
 248 order correction to the post-Keplerian parameters of binary systems.
 249 They find that the precession of the periastron is corrected by the
 250 parity-violating term. Using the measurements of the rate of peri-
 251 astron precession in the double pulsar system PSR J0737-3039 A/B,
 252 they obtain a constraint of $k_{\text{CS}}^{-1} \lesssim 0.4$ km, which corresponds to
 253 $M_{\text{PV}} \gtrsim 5 \times 10^{-10}$ eV. Note that the constraints of M_{PV} from the
 254 measurements of the Solar system and binary pulsar are based on the
 255 effect of frame-dragging modifications in the theory, which is the local
 256 effect rather than the propagation effect. Since the frame-dragging
 257 modification around rotating objects is a common feature for all parity-
 258 violating gravity models, although these constraints are derived for a
 259 specific parity-violating theory, i.e. Chern-Simons gravity, we expect
 260 that the conclusions are applicable for other theories of parity-violating
 261 gravity.

262
 263 Y.-F.W. thanks Badri Krishnan and Collin Capano for the fruitful
 264 discussion and acknowledges the Max Planck Gesellschaft for support
 265 and the Atlas cluster computing team at AEI Hannover. W.Z. and R.N.
 266 appreciate the helpful discussion with Linqing Wen, Xing Zhang, Qian
 267 Hu, Mingzheng Li and Anzhong Wang. W.Z. is supported by NSFC
 268 Grants No. 11773028, No. 11633001, No. 11653002, No. 11421303,

No. 11903030, and the Strategic Priority Research Program of the Chi-
 269 nese Academy of Sciences Grant No. XDB23010200. T.Z. is sup-
 270 ported in part by NSFC Grants No. 11675143, the Zhejiang Provin-
 271 cial NSFC Grant No. LY20A050002, and the Fundamental Research
 272 Funds for the Provincial Universities of Zhejiang in China Grants No.
 273 RF-A2019015. This research has made use of data, software and/or
 274 web tools obtained from the Gravitational Wave Open Science Cen-
 275 ter (<https://www.gw-openscience.org>), a service of LIGO Laboratory,
 276 the LIGO Scientific Collaboration and the Virgo Collaboration. LIGO
 277 is funded by the U.S. National Science Foundation. Virgo is funded
 278 by the French Centre National de Recherche Scientifique (CNRS), the
 279 Italian Istituto Nazionale della Fisica Nucleare (INFN) and the Dutch
 280 Nikhef, with contributions by Polish and Hungarian institutes.

281 Methods

282 In what follows we present our methods for inferring the con-
 283 straints on parity violation in gravity from GW measurements. We first
 284 introduce the construction of the parity-violating GW waveform in the
 285 EFT framework, then discuss the Bayesian inference for obtaining the
 286 constraints and forecast the constraints with future GW astronomy.

287 **GW waveform with parity violation** In this part we follow
 288 Refs.^{11,12,25} to briefly review the derivation of the GW waveform with
 289 parity-violation in the EFT framework. In the FRW universe, choosing
 290 the unitary gauge, the equation of motion of GW is determined by the
 291 following quadratic action¹¹

$$292 S = \frac{1}{16\pi G} \int dt d^3x a^3 \left[\frac{1}{4} \dot{h}_{ij}^2 - \frac{1}{4a^2} (\partial_k h_{ij})^2 + \right. \\ \left. \frac{1}{4} \left(\frac{c_1}{a M_{\text{PV}}} \epsilon^{ijk} \dot{h}_{il} \partial_j \dot{h}_{kl} + \frac{c_2}{a^3 M_{\text{PV}}} \epsilon^{ijk} \partial^2 h_{il} \partial_j h_{kl} \right) \right], \quad (3)$$

293 where the last two terms with three derivatives correspond to the contri-
 294 bution from parity violation. c_1 and c_2 are dimensionless coefficients,
 295 which are functions respective to cosmic time in general. Note that, in
 296 EFT, the leading-order modifications from parity-conserving terms in
 297 action are suppressed by M_{PV}^0 or M_{PV}^{-2} , which indicates the much
 298 looser constraint (or no constraint) of M_{PV} by GW observing these
 299 terms^{11,12,14}. From the action, we can derive the equation of motion of
 300 GW in the vacuum as shown in Eq. (1). The exact forms for μ_A and
 301 ν_A are¹²

$$302 \nu_A = [\rho_A \alpha_\nu(\tau)(k/a M_{\text{PV}})]' / \mathcal{H}, \\ \mu_A = \rho_A \alpha_\mu(\tau)(k/a M_{\text{PV}}), \quad (4)$$

303 where τ is the cosmic conformal time. The functions $\alpha_\nu \equiv -c_1$ and
 304 $\alpha_\mu \equiv c_1 - c_2$ are two arbitrary functions of time which can only be
 305 determined given a specific model of modified gravity. For the GW
 306 events at the local Universe, these two functions can be approximately
 307 treated as constant, i.e. ignoring their time-dependence. Note that we
 308 consider α_μ and α_ν to be $\sim \mathcal{O}(1)$ by absorbing the order of magnitude
 309 into M_{PV} . But a special case when $\alpha_\mu = 0$ (i.e., $c_1 = c_2 = 0$) for
 310 Chern-Simons gravity is also considered, the corresponding result is
 311 plotted in Fig. 1 as amplitude birefringence.

312 The explicit parity-violating GW waveform can be derived from
 313 solving the equation of motion, as schematically shown by Eq. (2).
 314 The amplitude and phase modifications to the GR-based waveform due
 315 to birefringence take the following parametrized form

$$316 \delta h(f) = -A_\nu \pi f, \quad \delta \Psi(f) = A_\mu (\pi f)^2 / H_0, \quad (5)$$

317 where H_0 is the Hubble constant. The coefficients A_ν and A_μ are given
 by

$$318 A_\nu = M_{\text{PV}}^{-1} (\alpha_\nu(z=0) - \alpha_\nu(z)(1+z)), \\ A_\mu = M_{\text{PV}}^{-1} \int_0^z \frac{\alpha_\mu(z')(1+z') dz'}{\sqrt{\Omega_M(1+z')^3 + \Omega_\Lambda}}, \quad (6)$$

where z is the redshift of the GW event. In analysis we adopt a Planck cosmology ($\Omega_M = 0.315$, $\Omega_\Lambda = 0.685$, $H_0 = 67.4$ km/s/Mpc)³³.

We also convert the left- and right-hand GW polarization modes into the *plus* and *cross* modes which are used more often in GW data analysis. The relation between the parity-violating modes and the GR modes is

$$\begin{aligned} h_+^{\text{PV}}(f) &= h_+^{\text{GR}}(f) - h_\times^{\text{GR}}(f)(i\delta h - \delta\Psi), \\ h_\times^{\text{PV}}(f) &= h_\times^{\text{GR}}(f) + h_+^{\text{GR}}(f)(i\delta h - \delta\Psi). \end{aligned} \quad (7)$$

The above expression represents the waveform we employ to compare with the GW data. Let us assume the GW is emitted at the redshift $z \sim O(0.1)$, and α_ν and α_μ are expected to be the same order constant, we find the ratio $\delta\Psi/\delta h \sim \pi f/H_0 \gtrsim 10^{20}$, where $f \sim 100$ Hz for the ground-based GW detectors. Therefore, in the general parity-violating gravity, except for the case with only amplitude birefringence (e.g. Chern-Simons modified gravity), the corrections of GW waveform $h^{\text{PV}}(f)$ mainly come from the contribution of velocity birefringence rather than that of amplitude birefringence.

Bayesian inference for GW events Bayesian inference framework is broadly employed in GW astronomy for estimating the source parameters and selecting the preferred model from observation. Given the data d of GW signal and a waveform model H , Bayes theorem claims

$$P(\vec{\theta}|d, H, I) = \frac{P(d|\vec{\theta}, H, I)P(\vec{\theta}|H, I)}{P(d|H, I)}, \quad (8)$$

where $\vec{\theta}$ are the parameters characterizing H , I is any other background information. $P(\vec{\theta}|H, I)$ is the prior distribution for $\vec{\theta}$ and $P(d|\vec{\theta}, H, I)$ is the likelihood for obtaining the data given a specific set of model parameters. The posterior $P(\vec{\theta}|d, H, I)$ contains all the information about the results of parameter estimation.

For the Gaussian and stationary noise from GW detectors, the likelihood function is

$$P(d|\vec{\theta}, H, I) \propto \exp\left[-\frac{1}{2} \sum_i \langle d - h(\vec{\theta}) | d - h(\vec{\theta}) \rangle\right], \quad (9)$$

where $h(\vec{\theta})$ is the GW waveform template in model H , and i represents the i -th GW detector. The inner product $\langle a|b \rangle$ is defined to be

$$\langle a|b \rangle = 4\Re \int \frac{a(f)b^*(f)}{S_h(f)} df, \quad (10)$$

where $S_h(f)$ is the one-side noise power spectral density (PSD) of the GW detector.

To select the model favored by observation, normalizing both sides of Eq. (8) and we can obtain the Bayes evidence

$$P(d|H, I) = \int d\vec{\theta} P(d|\vec{\theta}, H, I)P(\vec{\theta}|H, I). \quad (11)$$

Bayesian ratio is defined as the ratio of evidence between two competitive models H_1 and H_2 which are GR and parity-violating gravity within this work,

$$\mathcal{B}_2^1 = \frac{P(d|H_1, I)}{P(d|H_2, I)}. \quad (12)$$

The odds ratio between model H_1 and model H_2 can be expressed by

$$\mathcal{O}_2^1 = \frac{P(H_1|d, I)}{P(H_2|d, I)} = \frac{P(d|H_1, I) P(H_1|I)}{P(d|H_2, I) P(H_2|I)} = \mathcal{B}_2^1 \frac{P(H_1|I)}{P(H_2|I)}. \quad (13)$$

If the competitive models are assumed to be equally likely before any measurement, then odds ratio is equal to Bayesian ratio. Odds ratio quantitatively reflects the preference of data for competitive models.

We employ the open-source software `PYCBC` with the open data from¹⁸ to perform the Bayesian inference. For the GR waveform

$h^{\text{GR}}(f)$, we use the spin precessing waveform `IMRPhenomPv2`^{34,35} when analyzing BBH events and spin aligned waveform with tidal deformability added `IMRPhenomD_NRTidal`³⁶ for BNS events. The parity-violating waveform is constructed based on the above template through Eq.(7). We perform parameter estimation by selecting 16s data for BBH and 200s data for BNS events to account for the relatively long signal. The data is sampled at 2048 Hz and the likelihood is evaluated between 20 Hz and 1024 Hz. The PSD is generated from 1000s data using the median estimation with 8s Hann-windowed segments and overlapped by 4s¹⁹. The prior is chosen to be consistent with that of Ref.¹⁶ and uniformly distributed for A_μ and A_ν . The posterior distribution are sampled by the nest sampling algorithm `dynesty`³⁷ over the fiducial BBH and BNS source parameters plus the parity-violating parameters A_μ for velocity birefringence or A_ν for amplitude birefringence. Also note that, since we do not find any violation of GR and aim for putting a lower limit to M_{PV} , we ignore the calibration error from GW detectors, thus our lower limit should be interpreted as a conservative result for constraining M_{PV} . All the settings and parameter estimation results can be found in our released posterior files.

Fig. 2 shows the marginalized posterior distribution for A_μ for velocity birefringence. From the figure, we can observe that the GR value $A_\mu = 0$ is within the 90% confidence level for every event. We also report that the natural logarithm of the Bayes ratio between GR and the parity-violating gravity is distributed in the range [1.6, 5.8] for all the events, confirming no parity violation for gravity.

The relatively low-mass BBH events, such as GW151226, GW170608, and the two BNS events give tighter constraints on A_μ . This is because the velocity birefringence contribution corresponds to a 5.5 post-Newtonian (PN) order modification to the GR waveform which has larger impact on higher frequency, in line with the expectation that the low-mass events with higher cut-off frequency and longer signal yield better constraints.

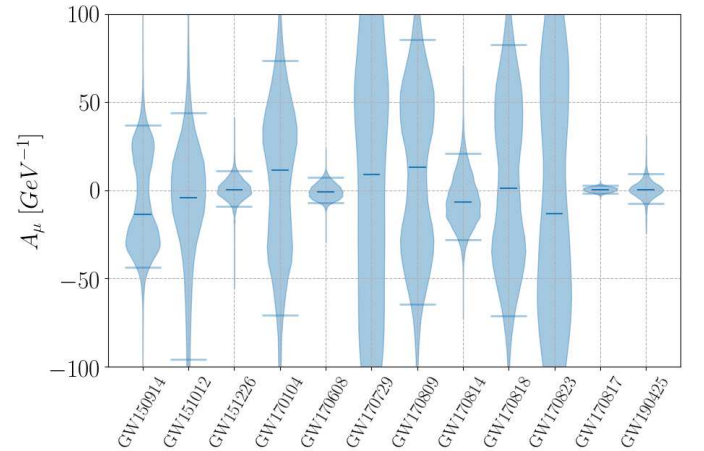


Figure 2 | Violin plots of the posteriors of the parameter A_μ The results are obtained by analyzing the twelve GW events. The region in the posterior between the upper and lower bar denote the 90% credible interval, and the bar at the middle denotes the median value. The GR value $A_\mu = 0$ is within the 90% confidence interval for each event. We notice that the two relative low-mass events GW151226 and GW170608 and the two BNS events yield the best constraint on A_μ .

For converting A_μ into M_{PV} , we absorb the absolute value of α_μ into the definition of M_{PV} , which is equivalent to set $|\alpha_\mu| = 1$ in the calculation, then the parameter M_{PV} can be obtained from A_μ and redshift z by Eq. (6). The marginalized posterior distributions of M_{PV} are shown in Fig. 3. It is straightforward to combine the posterior on M_{PV} from each event to give an overall constraint with all GW events

398 by

$$p(M_{\text{PV}}|\{d_i\}, H, I) \propto \prod_{i=1}^N p(M_{\text{PV}}|d_i, H, I), \quad (14)$$

399 where d_i denotes the i -th GW event. The combined result show that
 400 the 90% lower limit for M_{PV} is 0.09 GeV. This is the first observa-
 401 tional evidence of gravitational parity conservation from dynamical and
 402 strong-field observation and the tightest constraint on M_{PV} up to date.

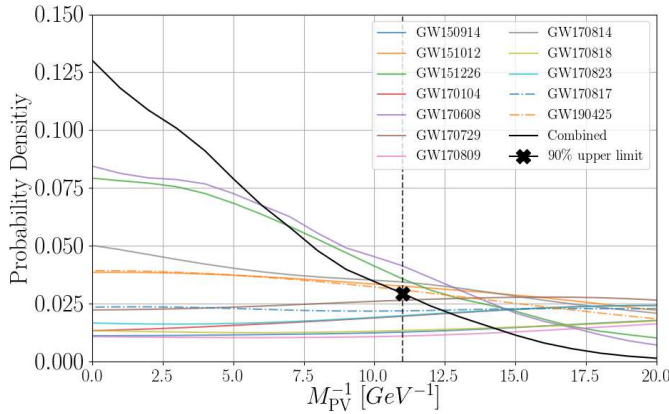


Figure 3 | The posterior distributions for M_{PV}^{-1} . The inference results for the parity-violating energy scale for velocity birefringence are plotted. The results from individual GW event and the combination of all the events are considered. The abscissa value of the “x” marker represents the 90% upper limit for M_{PV}^{-1} , or equivalently, the 90% lower limit for M_{PV} , which is 0.09 GeV.

403 **Testing parity of gravity in the high energy region with future**
 404 **GW detectors** We have shown that the current GW detection is capa-
 405 ble of probing the sub GeV parity-violating energy scale. With the
 406 continuing upgrade for GW detectors, we also forecast the ability of
 407 GW astronomy to constrain M_{PV} . We consider four sets of detector
 408 configurations based on technologies currently available or under in-
 409 vestigation, and simulate 200 BBH events from GR for each set. For
 410 the first set, we choose the advanced LIGO, advanced Virgo and KA-
 411 GRA network, all running with designed sensitivity. The second and
 412 third sets substitute the two LIGO detectors with the 2.5 generation
 413 detector A+³⁸ and the Voyager³⁹ configuration, respectively. The last
 414 set uses the third generation detectors including the Einstein Telescope^{27,40}
 415 and two Cosmic Explorer^{27,41} detectors located at the LIGO sites.

416 The simulated BBH events are uniformly located in the space and
 417 have mass uniformly distributed in the range $[5, 50]M_{\odot}$. For the first
 418 three sets, the upper cutoff for luminosity distance is chosen to be 2000
 419 Mpc, while for the third generation detectors the distance cutoff is 5000
 420 Mpc. We do not consider more distant sources to give a conservative
 421 estimation of the constraining ability of the future GW detector config-
 422 urations. We employ Bayesian inference to perform parameter estima-
 423 tion on the simulated events and choose the signal-to-noise ratio (SNR)
 424 > 8 as the criterion for detection.

425 In Fig. 4, we show the results of the combined constraints on M_{PV}
 426 with respect to the number of detections. We first notice that, out of
 427 the 200 sources, 40% of the sources can be detected by the advanced
 428 LIGO, advanced Virgo and KAGRA global network with design sensi-
 429 tivity, and M_{PV} can be constrained to 0.2 GeV, while the 2.5 gener-
 430 ation detectors A+ and Voyager can resolve 65% and 90% of sources,
 431 respectively, and constrain M_{PV} to be not less than 0.6 GeV and 1
 432 GeV.

433 For the last set of simulations, all the BBH sources can be detected
 434 by the third generation detectors, and the constraint with 200 events is
 435 10 GeV. Given the local merger rate estimation $53.2 \text{ yr}^{-1} \text{ Gpc}^{-3}$ from

LIGO and Virgo⁴², it is expected that there are $\mathcal{O}(10^4)$ BBH coales-
 436 cence events within 5000 Mpc in one year. Therefore, assuming the
 437 constraint on M_{PV} is inversely proportional to the square root of event
 438 number, the resultant constraint can reach $\mathcal{O}(10^2)$ GeV with a one-year
 439 observation with the third generation detectors. This demonstrates the
 440 promising future of GW astronomy to probe the ultraviolet property of
 441 gravity in the high energy region, which could shed light on deviations
 442 from GR, if exists, arising from the 100 GeV region.
 443

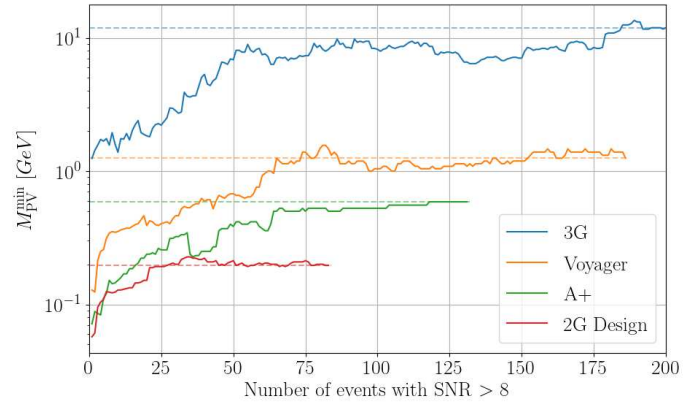


Figure 4 | The projected constraints for M_{PV} for future GW detectors. Using 200 BBH signals from GR, the constraints for the lower limit of the parity-violating energy scale for velocity birefringence are plotted. We consider four sets of global GW detectors network which are (1) the second generation detectors including advanced LIGO, advanced Virgo, and KAGRA with design sensitivity (2) the 2.5 generation detector A+ (3) the 2.5 generation detector Voyager (4) the third generation detector with the Einstein Telescope and Cosmic Explorer. As the number of detections increasing, the constraints for the lower limit of M_{PV} becomes tighter. In particular, the third generation detector can detect all the BBH coalescence signals within 5000 Mpc and can constrain $M_{\text{PV}} > \mathcal{O}(10)$ GeV with 200 events. With a one-year observation run, the third generation detectors are expected to improve the constraint to $\mathcal{O}(10^2)$ GeV.

Data availability The posterior files for velocity and amplitude birefringence of the twelve GW events are released in <https://yi-fan-wang.github.io/ParitywithGW/>

Code availability This work used the open-source software PyCBC which is available from <https://github.com/gwastro/pycbc>.

1. Lee, T. D. & Yang, C. N. Question of parity conservation in weak interactions. *Phys. Rev.* **104**, 254–258 (1956). URL <https://link.aps.org/doi/10.1103/PhysRev.104.254>.
2. Wu, C. S., Ambler, E., Hayward, R. W., Hoppes, D. D. & Hudson, R. P. Experimental test of parity conservation in beta decay. *Phys. Rev.* **105**, 1413–1415 (1957). URL <https://link.aps.org/doi/10.1103/PhysRev.105.1413>.
3. Alexander, S. & Yunes, N. Chern–simons modified general relativity. *Physics Reports* **480**, 1 – 55 (2009). URL <http://www.sciencedirect.com/science/article/pii/S037015730900177X>.
4. Crisostomi, M., Noui, K., Charmousis, C. & Langlois, D. Beyond love-lock gravity: Higher derivative metric theories. *Phys. Rev. D* **97**, 044034 (2018). URL <https://link.aps.org/doi/10.1103/PhysRevD.97.044034>.
5. Conroy, A. & Koivisto, T. Parity-violating gravity and GW170817 in non-riemannian cosmology. *Journal of Cosmology and Astroparticle Physics* **2019**, 016–016 (2019). URL <https://doi.org/10.1088/2F1475-7516%2F2019%2F12%2F016>.
6. Hořava, P. Quantum gravity at a lifshitz point. *Phys. Rev. D* **79**, 084008 (2009). URL <https://link.aps.org/doi/10.1103/PhysRevD.79.084008>.

7. Wang, A., Wu, Q., Zhao, W. & Zhu, T. Polarizing primordial gravitational waves by parity violation. *Phys. Rev. D* **87**, 103512 (2013). URL <https://link.aps.org/doi/10.1103/PhysRevD.87.103512>.
8. Miller, M. C. & Yunes, N. The new frontier of gravitational waves. *Nature* **568**, 469–476 (2019). URL <http://dx.doi.org/10.1038/s41586-019-1129-z>.
9. Yunes, N. & Siemens, X. Gravitational-wave tests of general relativity with ground-based detectors and pulsar-timing arrays. *Living Reviews in Relativity* **16** (2013). URL <http://dx.doi.org/10.12942/lrr-2013-9>.
10. Berti, E. *et al.* Testing general relativity with present and future astrophysical observations. *Classical and Quantum Gravity* **32**, 243001 (2015). URL <https://doi.org/10.1088%2F0264-9381%2F32%2F24%2F243001>.
11. Creminelli, P., Gleyzes, J., Noreña, J. & Vernizzi, F. Resilience of the standard predictions for primordial tensor modes. *Phys. Rev. Lett.* **113**, 231301 (2014). URL <https://link.aps.org/doi/10.1103/PhysRevLett.113.231301>.
12. Zhao, W., Zhu, T., Qiao, J. & Wang, A. Waveform of gravitational waves in the general parity-violating gravities. *Phys. Rev. D* **101**, 024002 (2020). URL <https://link.aps.org/doi/10.1103/PhysRevD.101.024002>.
13. Alexander, S. H. & Yunes, N. Gravitational wave probes of parity violation in compact binary coalescences. *Phys. Rev. D* **97**, 064033 (2018). URL <https://link.aps.org/doi/10.1103/PhysRevD.97.064033>.
14. Kostelecký, V. A. & Mewes, M. Testing local lorentz invariance with gravitational waves. *Physics Letters B* **757**, 510 – 514 (2016). URL <http://www.sciencedirect.com/science/article/pii/S0370269316301137>.
15. Abbott, B. P. *et al.* Tests of General Relativity with the Binary Black Hole Signals from the LIGO-Virgo Catalog GWTC-1 (2019). 1903.04467.
16. Abbott, B. P. *et al.* GWTC-1: A Gravitational-Wave Transient Catalog of Compact Binary Mergers Observed by LIGO and Virgo during the First and Second Observing Runs (2018). 1811.12907.
17. Abbott, B. P. *et al.* GW190425: Observation of a Compact Binary Coalescence with Total Mass $\sim 3.4M_{\odot}$ (2020). 2001.01761.
18. Vallisneri, M., Kanner, J., Williams, R., Weinstein, A. & Stephens, B. The LIGO Open Science Center. *J. Phys. Conf. Ser.* **610**, 012021 (2015). 1410.4839.
19. Biver, C. M. *et al.* PyCBC inference: A python-based parameter estimation toolkit for compact binary coalescence signals. *Publications of the Astronomical Society of the Pacific* **131**, 024503 (2019). URL <https://doi.org/10.1088%2F1538-3873%2Faaef0b>.
20. LIGO Scientific Collaboration. LIGO Algorithm Library - LALSuite. free software (GPL) (2018).
21. Yagi, K. & Yang, H. Probing gravitational parity violation with gravitational waves from stellar-mass black hole binaries. *Phys. Rev. D* **97**, 104018 (2018). URL <https://link.aps.org/doi/10.1103/PhysRevD.97.104018>.
22. Nair, R., Perkins, S., Silva, H. O. & Yunes, N. Fundamental Physics Implications for Higher-Curvature Theories from Binary Black Hole Signals in the LIGO-Virgo Catalog GWTC-1. *Phys. Rev. Lett.* **123**, 191101 (2019). 1905.00870.
23. Smith, T. L., Erickcek, A. L., Caldwell, R. R. & Kamionkowski, M. Effects of chern-simons gravity on bodies orbiting the earth. *Phys. Rev. D* **77**, 024015 (2008). URL <https://link.aps.org/doi/10.1103/PhysRevD.77.024015>.
24. Ali-Haïmoud, Y. Revisiting the double-binary-pulsar probe of nondynamical chern-simons gravity. *Phys. Rev. D* **83**, 124050 (2011). URL <https://link.aps.org/doi/10.1103/PhysRevD.83.124050>.
25. Zhao, W. *et al.* Model-independent test of the parity symmetry of gravity with gravitational waves. *Eur. Phys. J. C* **80**, 630 (2020). 1909.13007.
26. Abbott, B. P. *et al.* Prospects for Observing and Localizing Gravitational-Wave Transients with Advanced LIGO, Advanced Virgo and KAGRA. *Living Rev. Rel.* **21**, 3 (2018). 1304.0670.
27. Abbott, B. P. *et al.* Exploring the sensitivity of next generation gravitational wave detectors. *Classical and Quantum Gravity* **34**, 044001 (2017). URL <https://doi.org/10.1088%2F1361-6382%2Faa51f4>.
28. Abbott, B. *et al.* GW170817: Observation of Gravitational Waves from a Binary Neutron Star Inspiral. *Phys. Rev. Lett.* **119**, 161101 (2017). 1710.05832.
29. Abbott, B. P. *et al.* Gravitational waves and gamma-rays from a binary neutron star merger: GW170817 and GRB 170817a. *The Astrophysical Journal* **848**, L13 (2017). URL <https://doi.org/10.3847%2F2041-8213%2Faa920c>.
30. Nishizawa, A. & Kobayashi, T. Parity-violating gravity and gw170817. *Phys. Rev. D* **98**, 124018 (2018). URL <https://link.aps.org/doi/10.1103/PhysRevD.98.124018>.
31. Kostelecky, V. & Russell, N. Data Tables for Lorentz and CPT Violation. *Rev. Mod. Phys.* **83**, 11–31 (2011). 0801.0287.
32. Yunes, N. & Spergel, D. N. Double-binary-pulsar test of chern-simons modified gravity. *Phys. Rev. D* **80**, 042004 (2009). URL <https://link.aps.org/doi/10.1103/PhysRevD.80.042004>.
33. Aghanim, N. *et al.* Planck 2018 results. VI. Cosmological parameters (2018). 1807.06209.
34. Schmidt, P., Ohme, F. & Hannam, M. Towards models of gravitational waveforms from generic binaries: li. modelling precession effects with a single effective precession parameter. *Phys. Rev. D* **91**, 024043 (2015). URL <https://link.aps.org/doi/10.1103/PhysRevD.91.024043>.
35. Hannam, M. *et al.* Simple model of complete precessing black-hole-binary gravitational waveforms. *Phys. Rev. Lett.* **113**, 151101 (2014). URL <https://link.aps.org/doi/10.1103/PhysRevLett.113.151101>.
36. Dietrich, T., Bernuzzi, S. & Tichy, W. Closed-form tidal approximants for binary neutron star gravitational waveforms constructed from high-resolution numerical relativity simulations. *Phys. Rev. D* **96**, 121501 (2017). URL <https://link.aps.org/doi/10.1103/PhysRevD.96.121501>.
37. Speagle, J. S. dynesty: A dynamic nested sampling package for estimating bayesian posteriors and evidences. *Monthly Notices of the Royal Astronomical Society* (2020). URL <http://dx.doi.org/10.1093/mnras/staa278>.
38. <https://dcc.ligo.org/LIGO-T1800042/public>.
39. <https://dcc.ligo.org/LIGO-T1500293-v11/public>.
40. Punturo, M. *et al.* The einstein telescope: a third-generation gravitational wave observatory. *Classical and Quantum Gravity* **27**, 194002 (2010). URL <https://doi.org/10.1088%2F0264-9381%2F27%2F19%2F194002>.
41. Reitze, D. *et al.* Cosmic Explorer: The U.S. Contribution to Gravitational-Wave Astronomy beyond LIGO. *Bull. Am. Astron. Soc.* **51**, 035 (2019). 1907.04833.
42. Abbott, B. P. *et al.* Binary Black Hole Population Properties Inferred from the First and Second Observing Runs of Advanced LIGO and Advanced Virgo (2018). 1811.12940.

Figures

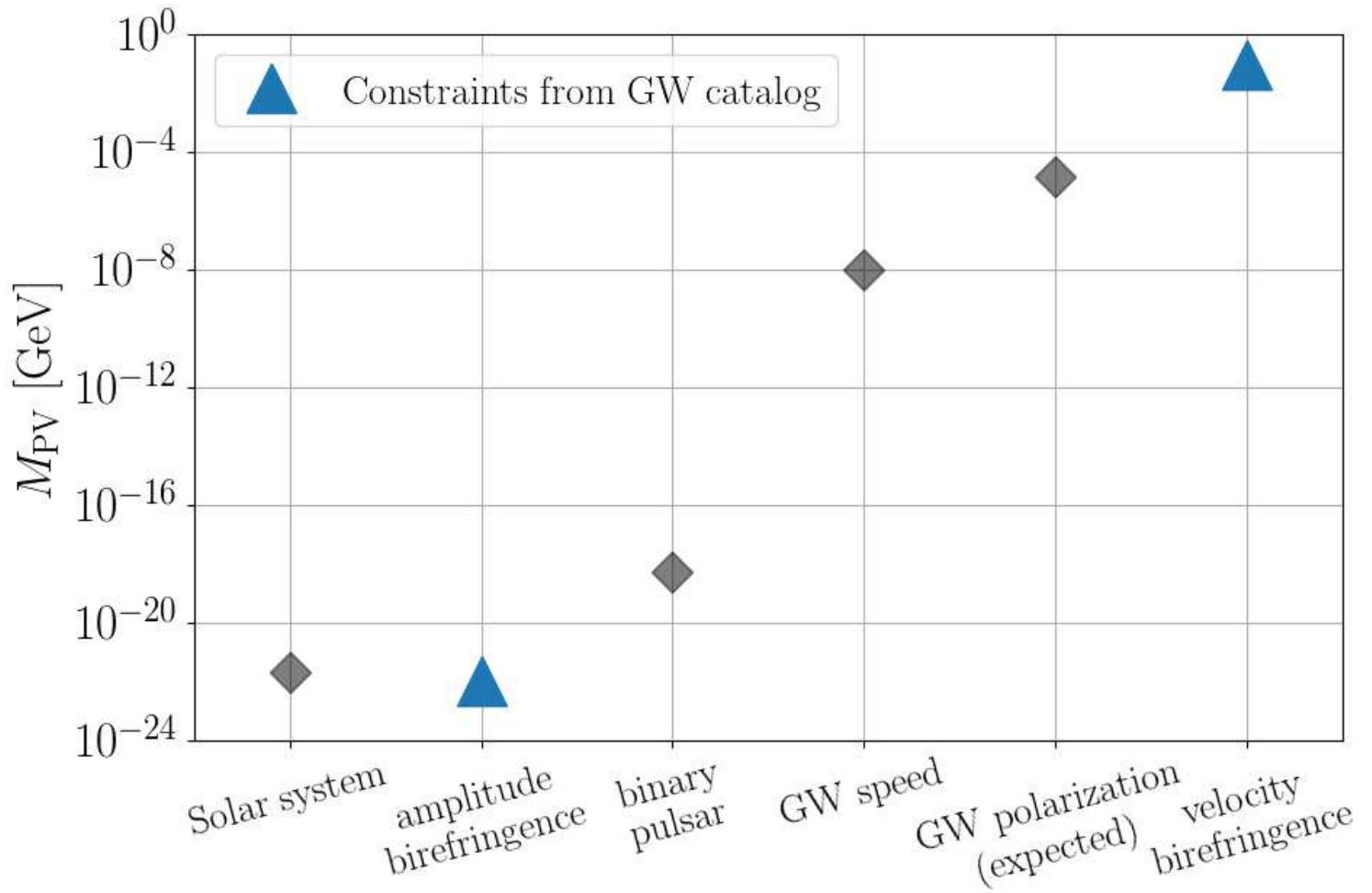


Figure 1

Current constraints on the lower limits of parity-violating energy scales in gravity from various observations. The triangle markers denote the constraints from the GW catalog for the general parity-violating gravity with velocity birefringence and the special case with only amplitude birefringence, respectively. For comparison, the figure also includes the results from the LAGEOS satellite in the Solar system 23, that from the double pulsar system PSR J0737-3039 A/B 24, that from the arrival time difference between GW170817 and GRB170817A, and the potential result by considering the waveform-independent method developed in Ref. 25.

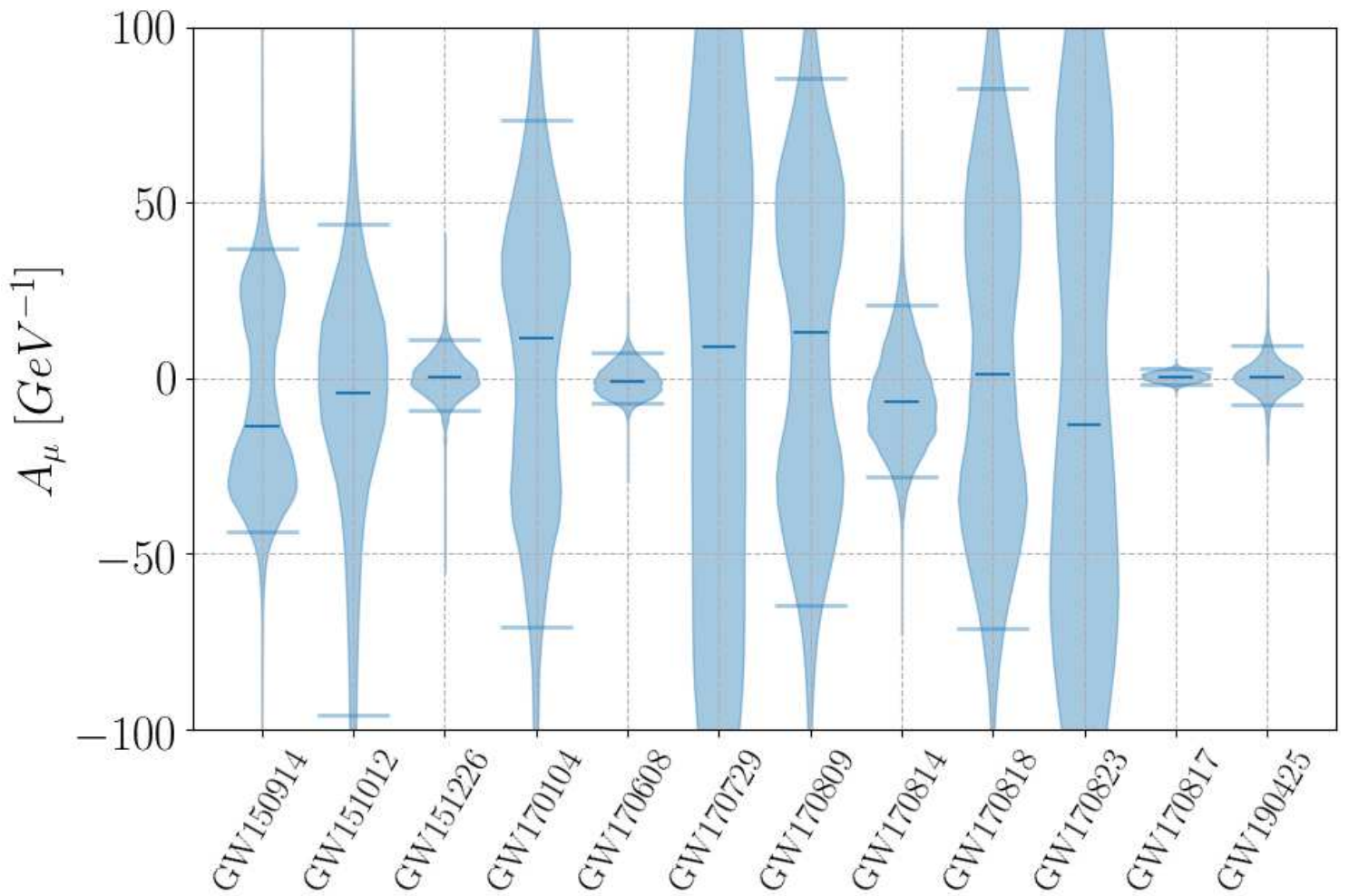


Figure 2

Violin plots of the posteriors of the parameter A_μ . The results are obtained by analyzing the twelve GW events. The region in the posterior between the upper and lower bar denote the 90% credible interval, and the bar at the middle denotes the median value. The GR value $A_\mu = 0$ is within the 90% confidence interval for each event. We notice that the two relative low-mass events GW151226 and GW170608 and the two BNS events yield the best constraint on A_μ .

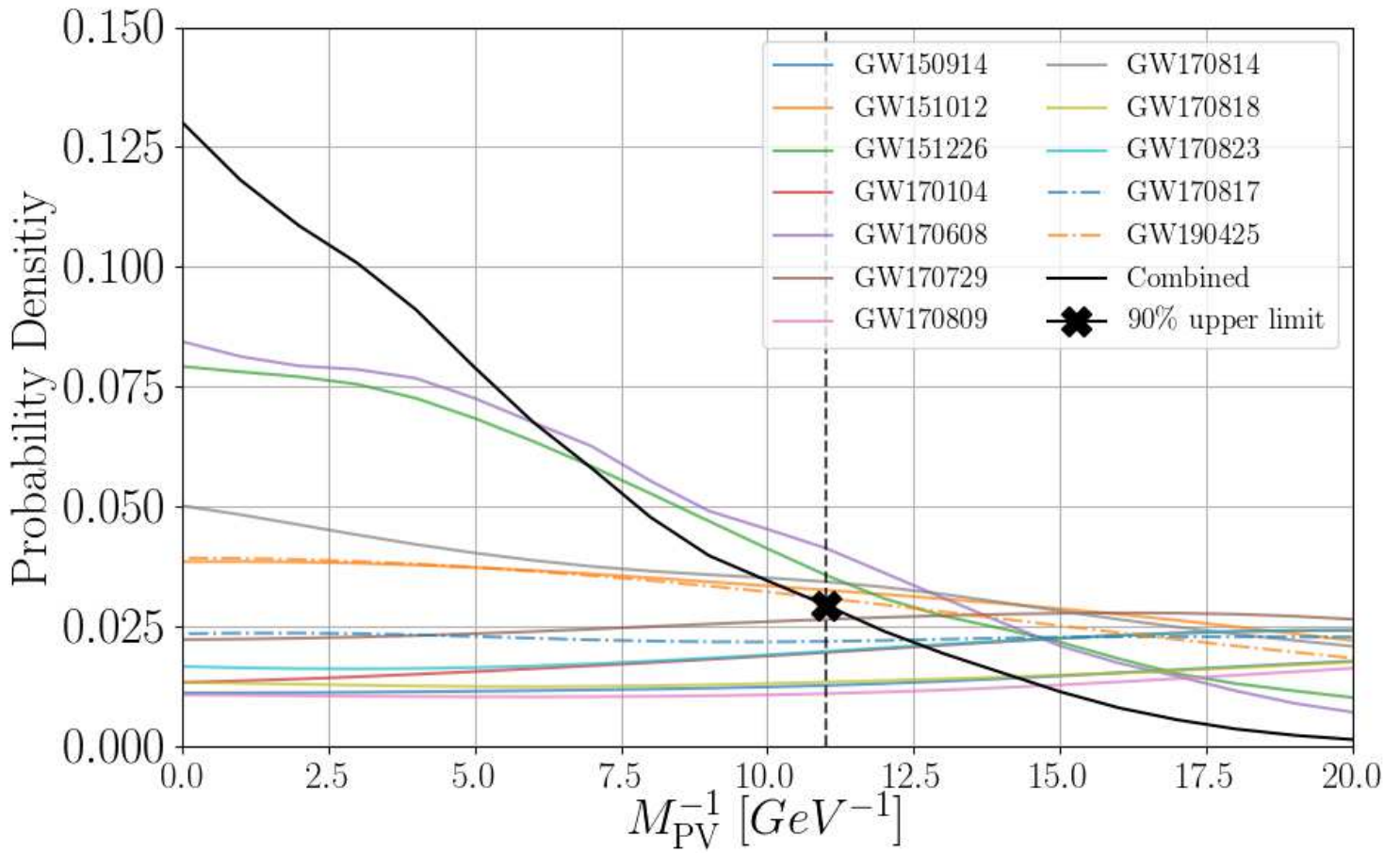


Figure 3

The posterior distributions for M^{-1}_{PV} . The inference results for the parity-violating energy scale for velocity birefringence are plotted. The results from individual GW event and the combination of all the events are considered. The abscissa value of the "x" marker represents the 90% upper limit for M^{-1}_{PV} , or equivalently, the 90% lower limit for M_{PV} , which is 0:09 GeV.

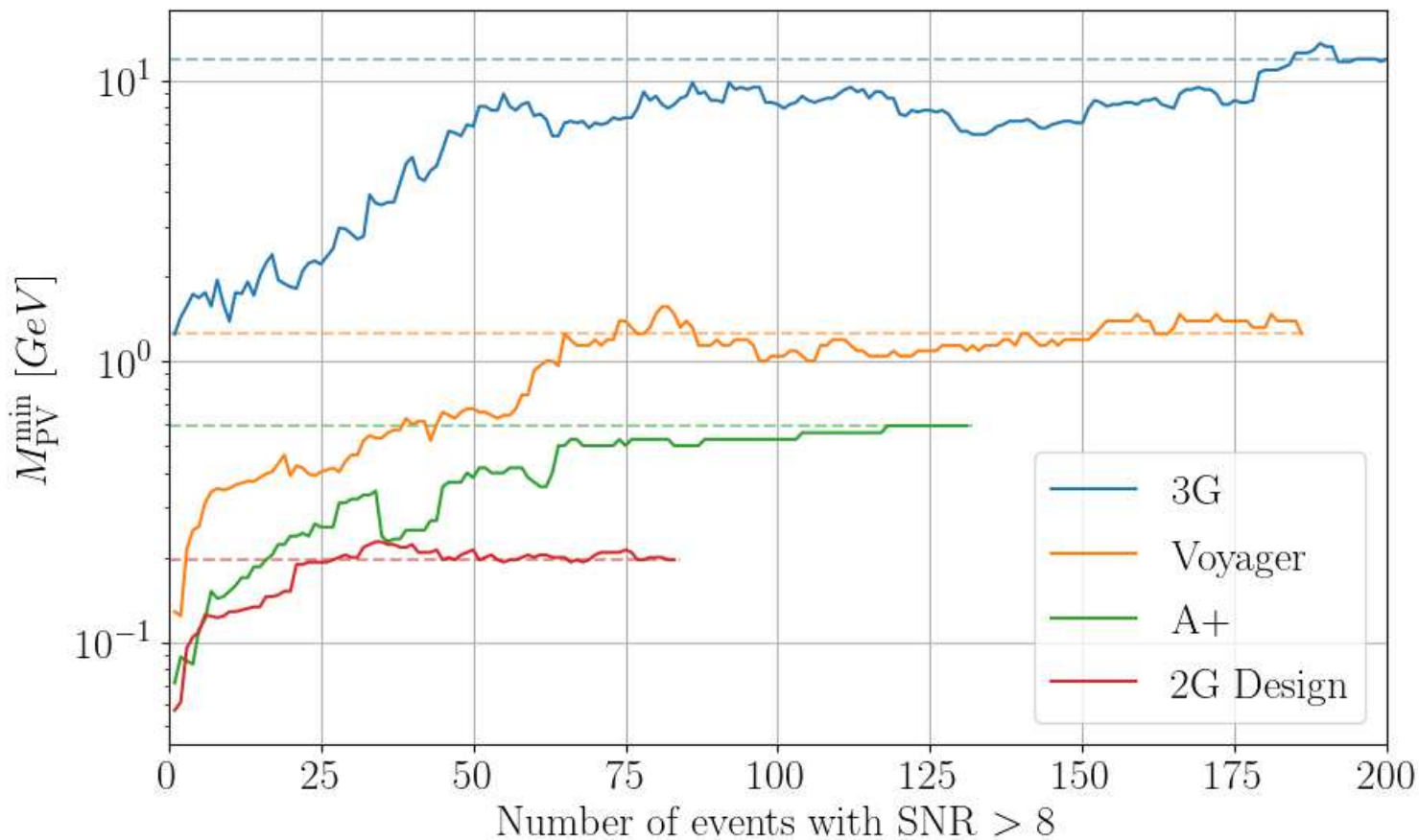


Figure 4

The projected constraints for MPV for future GW detectors. Using 200 BBH signals from GR, the constraints for the lower limit of the parityviolating energy scale for velocity birefringence are plotted. We consider four sets of global GW detectors network which are (1) the second generation detectors including advanced LIGO, advanced Virgo, and KAGRA with design sensitivity (2) the 2.5 generation detector A+ (3) the 2.5 generation detector Voyager (4) the third generation detector with the Einstein Telescope and Cosmic Explorer. As the number of detections increasing, the constraints for the lower limit of MPV becomes tighter. In particular, the third generation detector can detect all the BBH coalescence signals within 5000 Mpc and can constrain MPV > O(10) GeV with 200 events. With a one-year observation run, the third generation detectors are expected to improve the constraint to O(102) GeV.